Acta Biochim Biophys Sin 2025, 57(3): 403–414
https://cstr.cn/32197.14.abbs.2024168
https://doi.org/10.3724/abbs.2024168
Original Article

Original Article

Repurposed genipin targeting UCP2 exhibits antitumor activity through inducing ferroptosis in glioblastoma

Hao Dong[1,†], Kaixuan Sun[2,†], Xuejie Wang[1,†], Meimei Cui[1], Yaping Ma[1], Kexin Li[1], Wanli Duan[1], Hongxing Zhang[1], Liying Zhang[1], Zhimei Sheng[1], Maotao He[1,2,*], and Baogang Zhang[1,*]

[1]Department of Diagnostic Pathology, School of Basic Medical Sciences, Shandong Second Medical University, Weifang 261042, China, and [2]Department of Pathology, Affiliated Hospital of Shandong Second Medical University, Weifang 261041, China

[†]These authors contributed equally to this work

*Correspondence address. Tel: +86-15621605897; E-mail: hemaotao@wfmc.edu.cn (M.H.) / Tel: +86-18663684343; Email: zbg0903@hotmail.com (B.Z.)

Received 10 January 2024 Accepted 20 May 2024 Published 8 November 2024

Abstract

Uncoupling protein-2 (UCP2) controls the antioxidant response and redox homeostasis in cancer and is considered a potent molecular target for cancer treatment. However, the specific mechanism of UCP2 inhibition and its role in glioblastoma (GBM) have not yet been elucidated. Here, we attempt to identify a UCP2 inhibitor and study the underlying molecular mechanism in GBM. Bioinformatics analysis and immunohistochemistry are used to validate the high expression of UCP2 in GBM and its prognostic significance. Drug intervention and tumor xenograft experiments are conducted to determine the inhibitory effect of genipin, a UCP2 inhibitor, on UCP2. The mitochondrial membrane potential and key ferroptosis genes are examined to determine the occurrence of ferroptosis. High expression of UCP2 in GBM is associated with poor prognosis, and inhibiting UCP2 can alleviate the malignant behavior of GBM tumors. Genipin can downregulate the expression of GPX4 and upregulate the expression of ACSL4 by inhibiting UCP2, leading to ferroptosis and alleviating the malignant behavior of tumors. In summary, UCP2 is a potential therapeutic target for GBM. Genipin, which targets UCP2, effectively inhibits GBM development by inducing ferroptosis *in vivo* and *in vitro*. These findings indicate that genipin treatment based on UCP2 targeting has potential therapeutic applications with a clinical perspective for the treatment of GBM patients.

Key words genipin, uncoupling protein-2, ferroptosis, glioblastoma, malignant behavior of tumors

Introduction

Gliomas are tumors of the central nervous system that originate from glial cells, which are nonneural support cells of the brain. Gliomas account for 81% of intracranial tumors and are among the most common primary tumors in adults [1,2]. Glioblastoma (GBM) is the most aggressive and severe form of primary brain tumor and has a poor prognosis. Current treatment options include surgical resection, radiotherapy, and chemotherapy, but the survival rate for patients is low, with less than 5% of patients surviving beyond five years [3–5]. Therefore, identifying key molecules as therapeutic targets and developing effective targeted therapies to improve patient prognosis are crucial [6].

Uncoupling protein-2 (UCP2) belongs to the family of uncoupling proteins (UCPs) [7–9]. UCP2 acts as an antioxidant and inhibits the generation of reactive oxygen species (ROS) in mitochondria [10–12]. Essentially, tumor cells increase the expression of UCP2 to attenuate the cytotoxic effects of ROS by blocking the mitochondrial respiratory process [13]. The gene expression of UCP2 is regulated by various factors in the body. In general, UCP2 responds to unsaturated fatty acids to regulate energy metabolism [14,15]. Studies on UCP2 in tumors have indicated that it influences tumor metabolism through miRNA regulation [16,17]. Additionally, UCP2 is modulated by factors such as ROS, purine nucleotides, and coenzyme Q [11,18,19]. Undoubtedly, UCP2 is a novel metabolic therapeutic target. Research has shown that UCP2 expression is increased in various tumors [20–22]. Its roles in biochemical and physiological functions have been identified as follows: first, it protects cells from oxidative stress; second, UCP2 can modulate tumor progression through

alterations in glycolysis, oxidation, and calcium metabolism; and third, it can enhance antitumor immunity in the tumor microenvironment to restrict cancer development [23]. With these multiple intervention directions toward tumor cells, UCP2 can be considered a potential tumor treatment target.

Genipin is a product of geniposide hydrolysis by β-glucosidase and is an excellent natural biopolymer crosslinking agent [24–26]. Initially, genipin was used as a traditional herbal medicine for treating inflammation and jaundice and is also used as an edible coloring agent in some countries. Research has shown that genipin can inhibit UCP2 activity at the cellular level, making it a typical UCP2 inhibitor [27,28]. During tumorigenesis, genipin can attenuate ROS production by inhibiting UCP2, leading to ROS/c-Jun N-terminal kinase-dependent apoptosis in tumor cells. It also has the ability to inhibit AMP-activated protein kinase or NF-κB in the environment. By decreasing glycolytic flux and mitochondrial oxidative respiration, genipin reduces the tumorigenic effects of UCP2 by blocking its ability to dissipate energy through proton leakage and limiting ROS production. In simpler terms, genipin acts by inhibiting UCP2-mediated proton leakage, although the exact mechanism is still subject to debate.

Ferroptosis is an iron-dependent form of cell death triggered by the toxic accumulation of lipid peroxides on the cell membrane [29–31]. Altered ROS levels are also important indicators of ferroptosis [32,33]. It is a unique mode of cell death that is distinct from other programmed death modes and has significant potential in tumor therapy. The occurrence of ferroptosis implies the possibility of survival remission in cancer patients, indicating that ferroptosis is a significant direction for future tumor treatment [34–36]. Emerging evidence suggests that ferroptosis may play a crucial role in glioma development and progression.

The specific relationship between UCP2 and ferroptosis in gliomas is an area of active investigation. It is hypothesized that genipin, a typical UCP2 inhibitor, acts on mitochondria to inhibit the impact of UCP2 on ROS, triggering ferroptosis and reducing glioma progression. To elucidate this mechanism, we conducted a series of studies.

In this study, we evaluated the expression of UCP2 in gliomas and its prognostic significance and found a negative correlation between UCP2 expression levels and overall survival in glioma patients. Furthermore, the antitumor effects of *in vivo* and *in vitro* genipin treatment on glioma growth were assessed. These results demonstrated that genipin effectively inhibits the growth of GBM cells by suppressing UCP2-mediated ROS intervention and inducing ferroptosis.

Materials and Methods

Clinical specimens

Clinical GBM tissue samples were collected from patients who underwent surgical removal and were diagnosed with GBM according to the World Health Organization (WHO) pathological criteria at the Affiliated Hospital of Shandong Second Medical University. The pathological diagnosis of GBM was independently achieved by two senior and experienced pathologists. Ethical approval was obtained from the Affiliated Hospital of Shandong Second Medical University (approval number 2017202). Informed consent was obtained from each subject.

Immunohistochemical (IHC) staining

The experimental tissues were embedded in wax blocks, processed into sections, and immunohistochemically stained with specific antibodies against UCP2 (1:100, 11081-1-AP; Proteintech, Wuhan, China). The sections were then air-dried and mounted with neutral resin. Finally, the mounted slides were imaged and recorded under a BX51 optical microscope (Olympus, Tokyo, Japan).

Cell culture

LN-229 and U251 cells were obtained from American Type Culture Collection (ATCC). After successful revival, the culture mixture was replaced with fresh culture medium consisting of DMEM (Solarbio, Beijing, China) containing 10%FBS (Gibco, Waltham, USA) in a laminar flow hood and further cultured in a CO_2 incubator at 37°C with 5% CO_2.

Western blot analysis

The cells were lysed to obtain the desired proteins according to the methods described in a previous report [37]. Then, the protein samples were subject to SDS-PAGE (12% separating gel and 5% stacking gel) and transferred to PVDF membranes (IPFL00010; Merck KGaA, Darmstadt, Germany), and 5% skim milk was used to block the membranes. Membranes were washed with TBST and incubated with the corresponding primary antibody UCP2 (1:1000, 89326; CST, Danvers, USA), T-cadherin (1:100, sc-166875; Santa Cruz Biotechnology, Shanghai, China), N-cadherin (1:2000, 22018-1-AP; Proteintech), AKT (1:2000, 9272; CST), p-AKT, (1:2000, 4060; CST), BAX (1:10000, 50599-2-Ig; Proteintech), Bcl-2 (1:4000, 68103-1-Ig; Proteintech), GPX4 (1:3000, 67763-1-Ig; Proteintech), ACSL4 (1:3000, 66617-1-Ig; Proteintech) overnight at 4°C. The next day, the membranes were washed and incubated with the corresponding secondary antibody (1:5000; Proteintech) in TBST atroom temperature for 1 h. After being rinsed with TBST, the membranes were detected using an enhanced chemiluminescent substrate solution (P0018FS; Beyotime, Shanghai, China), and images were captured with an ultra-sensitive multifunctional imager (ImageQuant 800 Fluor; Amersham, Cytiva, USA).

Cell proliferation and cytotoxicity assay

In a 96-well plate, the cells were seeded and incubated for at least 12 h. Then, different concentrations of genipin (G4796; Merck KGaA) and other reagents were added. After further culture for a period of time, cell growth was assessed via the MTT Cell Proliferation and Cytotoxicity Assay Kit (M1020; Solarbio). The absorbance value of each well was measured at 490 nm on a microplate photometer (1410101; Thermo Fisher Scientific, Waltham, USA). Three replicates were set for each group, with three wells per replicate.

Colony formation assay

For the colony formation assay, 1000 cells were inoculated per Petri dish, and the cells were cultured for approximately two weeks. Paraformaldehyde (4%) was used to fix the colonies, and crystal violet (G1062; Solarbio) was used for staining. The colonies were counted using Quantity One software (Bio-Rad, Hercules, USA). Each group was repeated three times.

EdU assay

Cell proliferation was detected via an EdU Cell Proliferation Assay Kit (C0071S; Beyotime). The cells were cultured in a 24-well plate for 24 h to allow them to fully adhere to the glass slides. EdU

working solution was added to the treated cells, which were then incubated for 4 h. Then, the instructions of the kit were followed for further experimentation (avoiding exposure to light during this period). Finally, the glass slides were removed, Hoechst solution was added, and the samples were incubated in the dark for 10 min. Images were captured via a BX53M fluorescence microscope (Olympus). The experiment was repeated three times per group.

Wound healing assay

Wound healing assay was performed via the use of 10 μL pipette tips to scrape cells in 6-well plates to produce vertical wounds. The cells were cultured in medium containing only 1% FBS to exclude the effect of cell proliferation. After the cells were treated with different concentrations of genipin, images of the wound area were taken at 0, 24, and 48 h using the BX51 optical microscope. Representative boundaries of the wounds were drawn with straight lines. Wound size was quantified by ImageJ (version 1.53e). Each set of experiments was repeated three times.

Transwell assay

Glioma cells were cultured for 24 h, digested with trypsin for counting, and resuspended in serum-free medium. About 1×10^4 cells (200 μL) were seeded to the upper chamber of the Transwells (Corning, Corning, USA) in 24-well plates, and 600 μL of complete medium containing 10% FBS was added to the lower chamber for the experiment. Then, cells were cultured in an incubator at 37°C and 5% CO_2 for 24 h. The migrated cells in the Transwell chamber were fixed with 4% paraformaldehyde, and stained with Giemsa (G8220; Solarbio). Images were taken via the BX51 optical microscope, and the number of cells was counted.

Oligo siRNA

The experiments were carried out in 6-well plates with 0.5×10^6 cells per well. The experiment was started when the growth density of the tumor cells was approximately 70%. First, 50 μL of OPTI-MEM (GenePharma, Shanghai, China) was added to 1.5-mL sterile centrifuge tubes with the appropriate amount of transfection reagent, gently mixed via a pipette, and left to stand for 5 min at room temperature; 50 μL of OPTI-MEM was added to another batch of 1.5-mL sterile centrifuge tubes with an appropriate amount of RNA oligo, gently mixed via a pipette, and left to stand for 5 min at room temperature; at the end of the resting period, the GP-transfect-Mate medium mixture was added dropwise into the RNA oligo medium mixture, mixed gently with a pipette, and allowed to stand at room temperature for 15 min. Transfection was then carried out immediately. After that, the cells were incubated in an incubator at 37°C with 5% CO_2. Six hours later, the culture medium were refreshed and cells were incubated again at a constant temperature for 48 h before subsequent experiments were carried out. The sequences of the siRNAs used to target *UCP2* are listed in Table 1.

JC-1 assay

The glass slides and the appropriate amount of tumor cells were cultured in a 24-well plate. The experiments were conducted according to the manufacturer's instructions for the JC-1 staining (C2006; Beyotime). After completion, the glass slides were removed and fixed onto microscope slides. The samples were observed under the BX53M fluorescence microscope, and images were captured. The experiment was repeated three times.

Table 1. Sequences of the siRNAs used in this study

Name	Sequence
siUCP2#1	Sense, 5′-GUGGUCAAGACGAGAUACATT-3′ Antisense, 5′-UGUAUCUCGUCUUGACCACTT-3′
SiUCP2#2	Sense, 5′-CUGCUAAAGUCCGGUUACATT-3′ Antisense, 5′-UGUAACCGGACUUUAGCAGTT-3′
siUCP2#3	Sense, 5′-GAUUCUGUCAAACAGUUCUTT-3′ Antisense, 5′-AGAACUGUUUGACAGAAUCTT-3′
siRNA NC	Sense, 5′-UUCUCCGAACGUGUCACGUTT-3′ Antisense, 5′-ACGUGACACGUUCGGAGAATT-3′

Animal experiment

Eighteen male nude mice (4 weeks old; Jinan Pengyue Experimental Animal Breeding Co., Ltd, Jinan, China) were selected for the experiment, and the mice were kept in a mouse facility with a cycle of 12 h of light and 12 h of darkness for one week of acclimatization. All procedures were approved by the Animal Care and Use Committee of Jinan Pengyue Experimental Animal Breeding Co., Ltd and conformed to legal mandates and National Guidelines for the Care and Maintenance of Laboratory Animals. LN-229 glioma cells at the logarithmic stage were subcutaneously implanted into nude mice. Tumor growth was observed one week after injection. When tumor diameter was approximately 4 mm at two weeks, genipin drug injection (55 mg/kg) and negative control injection of DMSO were performed. The weight and volume were recorded every 4 days. After 35 days, mice were sacrificed and the tumors were collected for subsequent experiments. The formula for tumor volume calculation was: $[(\text{short diameter})^2 \times (\text{long diameter})]/2$.

Statistical analysis

All experimental measurements in this study were repeated at least three times, and data are expressed as the mean±standard deviation (SD). A *t* test was used to compare the means of the two groups. All the statistical analyses were performed via GraphPad Prism. $P<0.05$ was considered statistically significant.

Results

UCP2 is highly expressed in GBM and negatively correlates with patient survival

To investigate the clinicopathological characteristics of UCP2 in human glioblastoma (GBM), immunohistochemical staining was performed on normal human brain tissues and tumor tissues from GMB patients. The results revealed significantly increased expression levels of UCP2 in GBM tissues (Figure 1A). Database analysis revealed that GBM patients with high UCP2 expression had shorter survival periods and poorer prognoses than those with low UCP2 expression (Figure 1B). The high expression of UCP2 in GBM paralleled that in other common malignancies (Figure 1C,D and Supplementary Figure S1A,B), and its expression appeared to be positively correlated with stage in GBM (Supplementary Figure S1C). Moreover, UCP2 is expressed at higher levels in wild-type GBM (Supplementary Figure S1D), but it is not associated with the age or sex of GBM patients (Supplementary Figure S1E,F). Furthermore, UCP2 was found to be highly expressed in GBM patients without 1p/19q codeletion (Supplementary Figure S2A), and this expression was closely linked to the stage of GBM patients (Supplementary Figure S2B), further establishing UCP2 as a predictor of poor prognosis in GBM patients.

To evaluate the functional role of UCP2 in GBM, LN-229 and U251

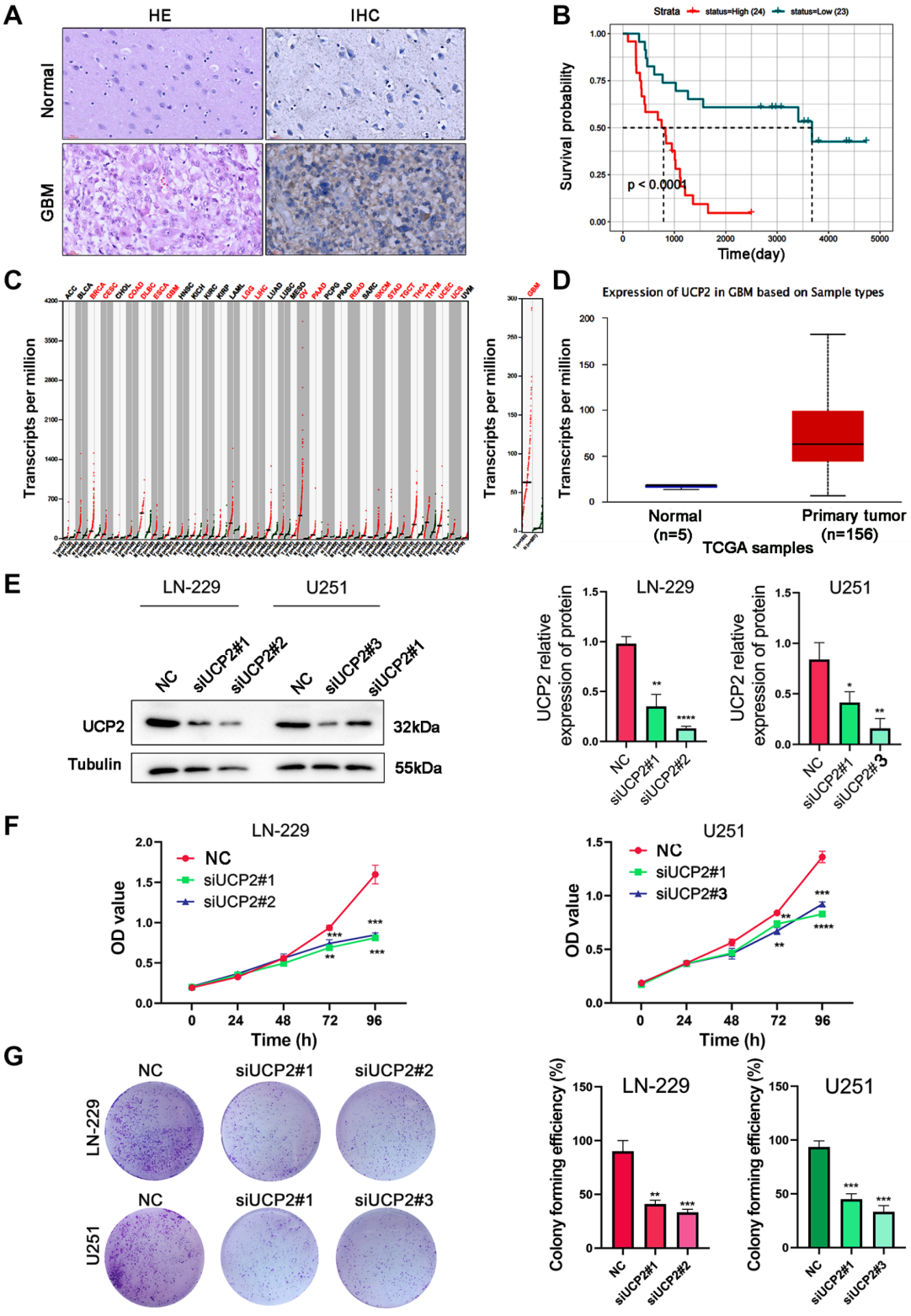

Figure 1. UCP2 is highly expressed in GBM and negatively correlates with the probability of patient survival (A) HE and IHC were used to assess UCP2 expression levels in GBM and normal samples. (B) The survival of patients with high UCP2 expression in GBM was queried via bioinformatics databases. (C) Biodata showing UCP2 expression in major tumors. (D) UCP2 expression in GBM. (E) *UCP2* knockdown efficiency in LN-229 and U251 cells. Oligo-mediated *UCP2* knockdown. UCP2 expression was detected by western blot analysis. (F) Cell viability was determined by the MTT assay in the *UCP2*-knockdown LN-229 and U251 cell lines at the indicated time points. (G) Colony formation of LN-229 and U251 cells after *UCP2* knockdown. Data are presented as the mean±SD from independent experiments. $^{*}P < 0.05$, $^{**}P < 0.01$, $^{***}P < 0.001$.

cell lines with *UCP2* gene knockdown were established via Oligo technology (Figure 1E). As expected, the knockdown of *UCP2* in LN-229 and U251 cells hindered cell proliferation (Figure 1F). Additionally, the results of the cell colony formation experiments demonstrated that GBM cells with low UCP2 expression presented weaker colony formation ability (Figure 1G). These findings suggest that UCP2 plays a role in promoting cell proliferation and tumor growth in GBM.

Genipin suppresses cell proliferation by inhibiting UCP2 in GBM cells

To investigate whether genipin can inhibit UCP2 and exert effects on GBM cells, we initially treated LN-229 and U251 cells with genipin and observed changes in their protein levels. The results showed that genipin treatment significantly reduced the expression of UCP2 in GBM cells (Figure 2A,B). Additionally, genipin exhibited an increasing inhibitory effect on cell survival over time (Figure 2C,D). The findings confirmed that genipin induced a dose- and time-dependent reduction in glioblastoma cell numbers (Figure 2G,H). Moreover, the cell morphology gradually became more spherical, indicating a deterioration of cell health and potential onset of cell death (Figure 2E,F). The proliferation of LN-229 and U251 cells was significantly inhibited after genipin treatment (Figure 2I,J). These findings collectively suggest that genipin suppresses UCP2 and reduces the proliferation of GBM cells.

Genipin inhibits migration and invasion by inhibiting UCP2 in GBM cells

To investigate the effects of genipin on migration and invasion, wound healing and transwell assays were performed. The results revealed a significant reduction in the migration of both types of GBM cells following genipin treatment (Figure 3A). Similarly, the transwell assay demonstrated a significant decrease in cell invasiveness (Figure 3B), which was consistent with observations in *UCP2*-silenced GBM cells (Supplementary Figure S3A,B). Western blot analysis revealed that genipin-mediated UCP2 inhibition led to downregulation of the AKT signaling pathway, a mediator of cell proliferation (Figure 3E).

Furthermore, the expressions of proteins related to epithelial-mesenchymal transition (TME) were examined. Genipin treatment resulted in a significant increase in the intracellular T-cadherin protein level (Figure 3C) and a marked reduction in N-cadherin expression (Figure 3D), indicating its potential anti-invasive action. Additionally, a decrease in vimentin protein expression was observed, further supporting the role of genipin in reducing the invasive and migratory abilities of glioblastoma cells (Supplementary Figure S3C–E). Moreover, genipin caused a reduction in the Bcl2/BAX ratio, promoting apoptotic processes in GBM cells (Figure 3F), suggesting that genipin may induce glioma cell death, partially via apoptotic pathways. In summary, these findings demonstrate that genipin suppresses the malignant behavior of GBM cells by targeting UCP2.

Genipin induces ferroptosis by inhibiting UCP2 and increasing ROS in GBM cells

To investigate the mechanism underlying the potent inhibition of GBM cell growth by genipin, we focused on the role of UCP2 and its inhibition by genipin. Our findings suggest that genipin inhibits UCP2, leading to the inhibition of UCP2-mediated proton leakage and potentially enabling a new role for ROS (Figure 4A). On the basis of this information, we hypothesized that the inhibition of UCP2 by genipin may affect the mitochondrial membrane potential and increase the production of ROS, thereby triggering ferroptosis in GBM cells.

We first used JC-1 to observe changes in the mitochondrial membrane potential. Compared with the control group, the genipin group presented significantly stronger green fluorescence (Figure 4B). Western blot analysis revealed a significant decrease in the protein level of the ferroptosis negative regulatory factor GPX4 and a significant increase in the protein level of the positive regulatory factor ACSL4 in glioblastoma cells treated with genipin (Figure 4C,D). To exclude potential confounding effects of genipin on experimental accuracy, we replicated the aforementioned experiments utilizing siUCP2. The results demonstrated that *UCP2* knockdown significantly decreased the protein level of GPX4 in glioma cells (Supplementary Figure S4A,B) and correspondingly increased the protein level of ACSL4 (Supplementary Figure S4C,D). Collectively, these outcomes consistently point to the induction of ferroptosis. NAC is a scavenger of lipid reactive oxygen species (ROS) and an inhibitor of iron deficiency anemia. NAC intervention has been shown to rescue GBM cell death (Figure 5A). Furthermore, we treated GBM cells with ferrostatin-1 (Fer-1), a known iron deficiency inhibitor, and found that Fer-1 effectively prevented iron depletion (Figure 5B). In contrast, RSL3, an iron depletion inducer, exacerbated iron deficiency. (Figure 5C). In summary, the promotion of GPX4-mediated ferroptosis by genipin is correlated with ROS production, which may contribute to the inhibition of GBM cell proliferation.

Genipin suppresses GBM tumor development *in vivo*

To evaluate the antitumor efficacy of genipin *in vivo*, we treated nude mice with genipin. First, we subcutaneously injected a sufficient quantity of human LN-229 glioma cells in the logarithmic growth phase into the skin of nude mice. After the cells had formed subcutaneous tumors and reached the desired size, we injected an intraperitoneal genipin solution in the genipin group and an equal volume of DMSO in the DMSO group (Figure 6A). After 35 days, we euthanized the mice to harvest the tumor tissues, and the size and morphology of the tumors are depicted in the figure (split into two operations) (Figure 6B). Notably, compared with DMSO treatment, genipin treatment resulted in a significant reduction in tumor volume (Figure 6C). The tumor weights were also significantly lower in the genipin-treated mice (Figure 6D), indicating stronger tumor suppression in the genipin group (Figure 6E). Importantly, histological analysis of other body tissues via hematoxylin and eosin (HE) staining revealed no adverse effects of genipin (Figure 6F). Furthermore, we assessed the expression levels of ferroptosis-related proteins in the four groups of tumor tissue. The results revealed that UCP2 level was significantly reduced in the genipin group; whereas the expression of GPX4, a negative regulator of ferroptosis, was considerably decreased; conversely, ACSL4, a positive regulatory protein, was markedly increased (Figure 6G). Overall, these results indicate that genipin reduces the growth of GBM tumors *in vivo*. These findings suggest that genipin has a positive effect on gliomas by inhibiting the growth and proliferation of glioma cells through the ferroptosis pathway, thereby slowing glioma development. These findings provide a valuable theoretical basis for future glioma treatments.

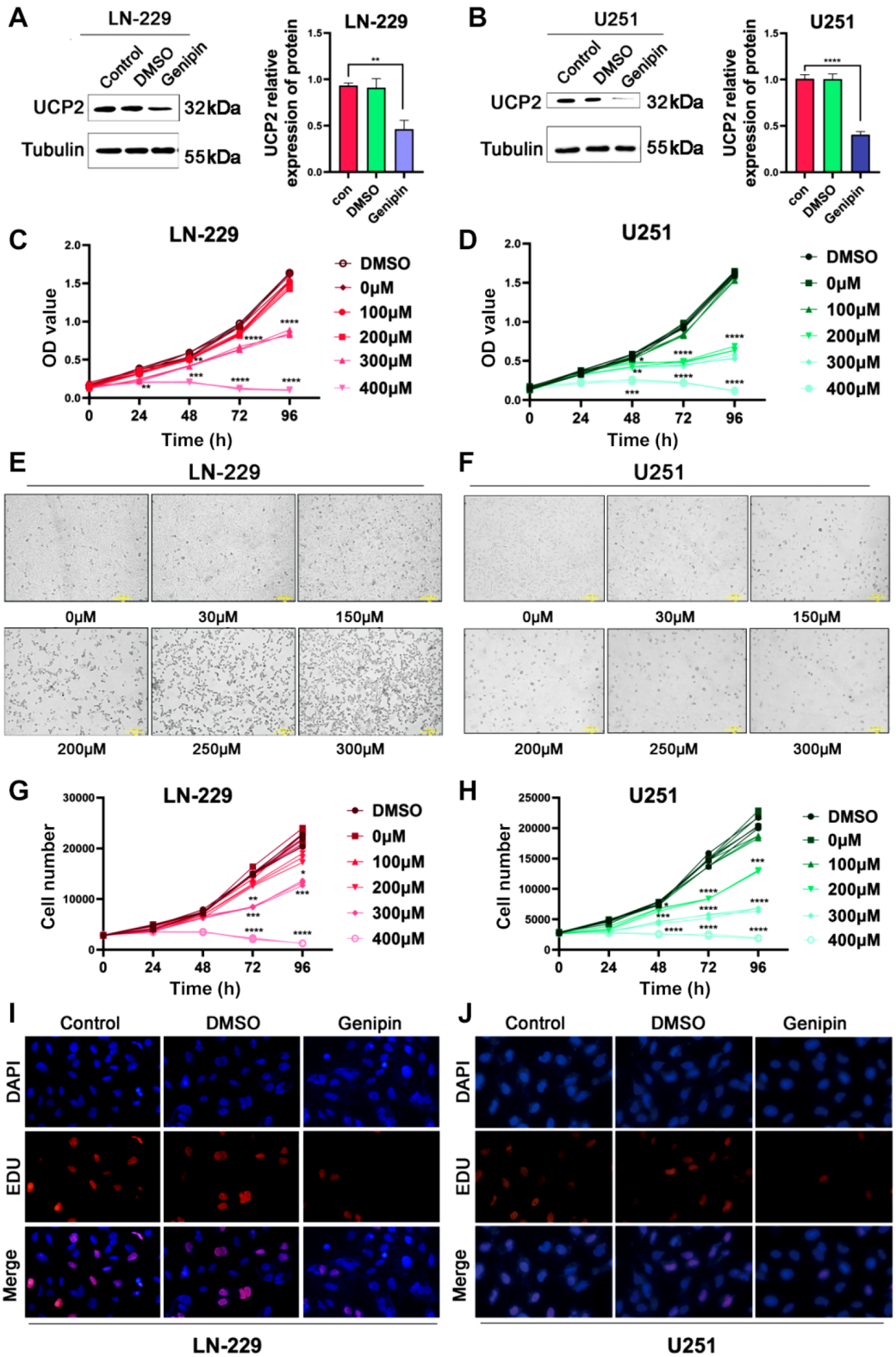

Figure 2. Genipin suppresses cell proliferation by inhibiting UCP2 in GBM cells (A,B) Changes in the protein levels of UCP2 after genipin intervention in GBM cells with DMSO concentrations exceeding the normal tolerance range were used as an experimental group to observe whether DMSO had an effect on the experiments. (C,D) Detection of cell growth viability after genipin intervention in GBM cells. (E–H) LN-229 and U251 cells were treated with different doses of genipin (0, 100, 200, 300, or 400 μM), and cell counts were determined. Cell growth status was recorded at 0, 24, 48, 72, and 96 h. (I,J) Changes in cell proliferation capacity were detected via the EDU fluorescence technique after genipin intervention in GBM cells. $^{*}P < 0.05$, $^{**}P < 0.01$, $^{***}P < 0.001$.

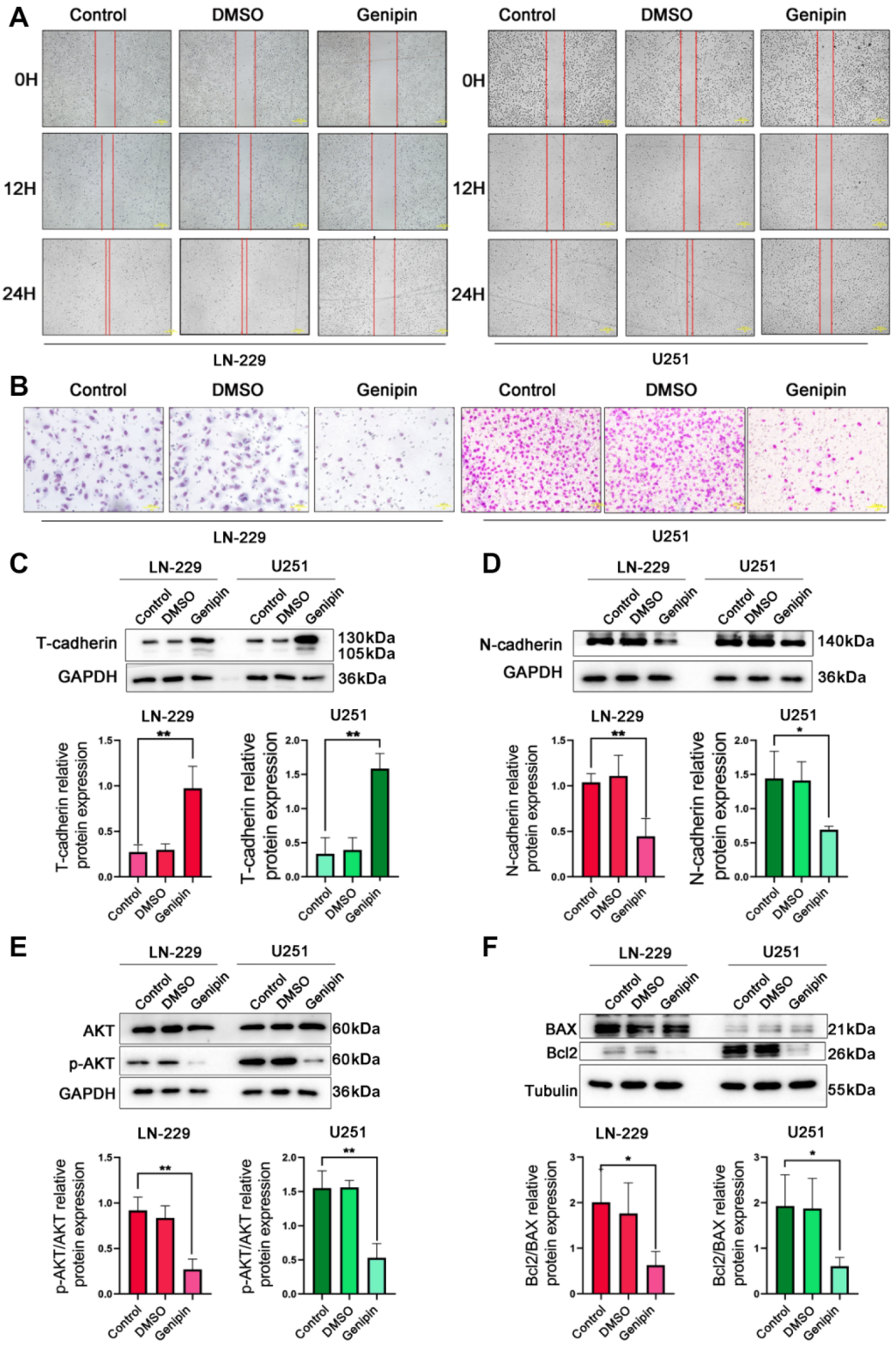

Figure 3. Genipin inhibits migration and invasion by inhibiting UCP2 in GBM cells (A) The migration ability of GBM cells after treatment with genipin was detected via a cell scratch assay. (B) Transwell assays demonstrated the invasive ability of GBM cells after genipin intervention. (C) Changes in the protein level of T-cadherin after the action of genipin on GBM cells. (D) Changes in the protein level of N-cadherin in GBM cells after treatment with genipin. (E) Changes in the level of the AKT protein in GBM cells after treatment with genipin. (F) Changes in the Bcl2/BAX protein level after genipin intervention in GBM cells. $*P < 0.05$, $**P < 0.01$.

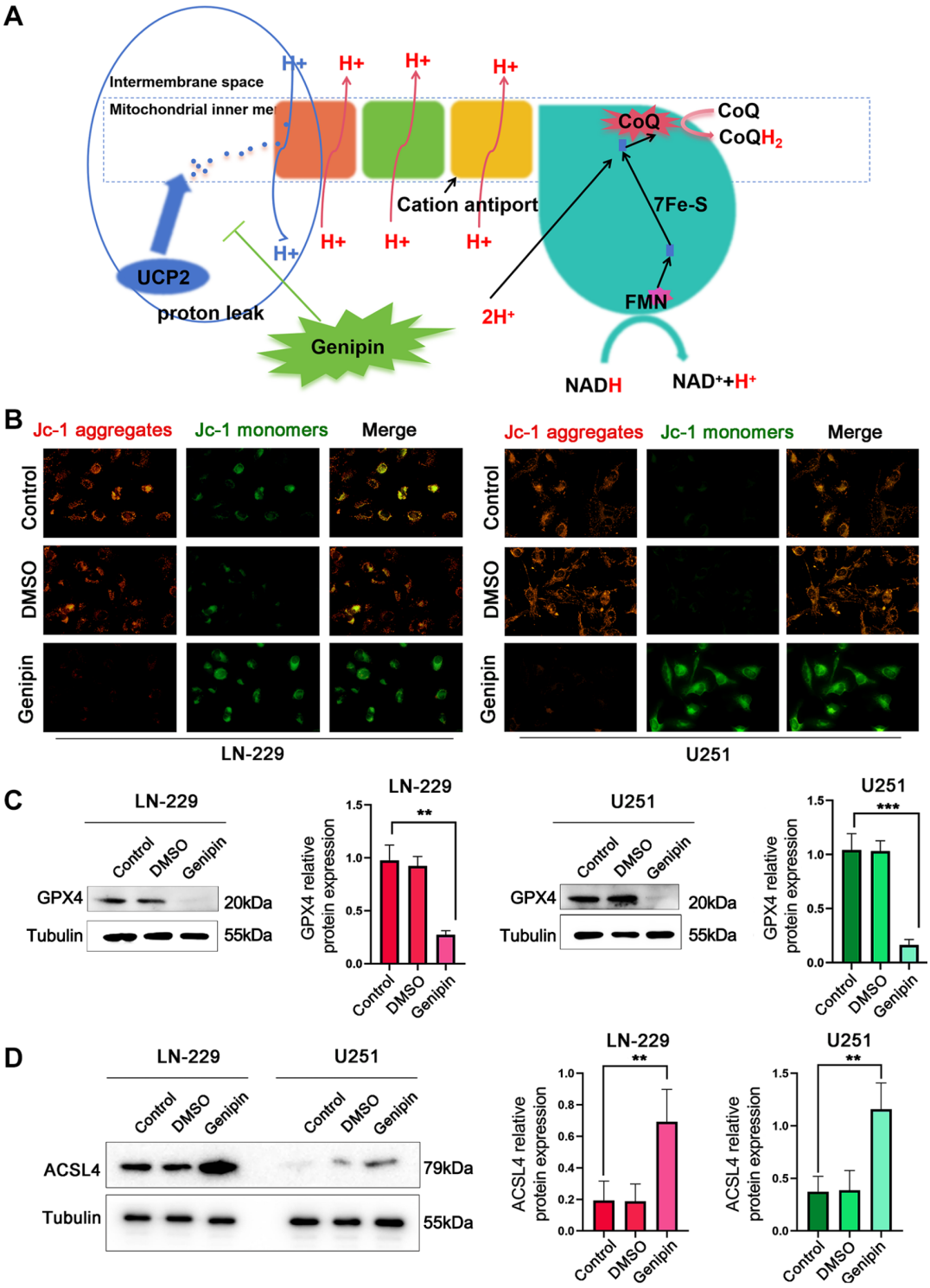

Figure 4. Genipin induces ferroptosis by inhibiting UCP2 in GBM cells (A) Mapping of the intrinsic mechanism of UCP2 inhibition by genipin. (B) Alteration of the mitochondrial membrane potential in GBM cells after inhibition of UCP2 by genipin. (C) Changes in the protein level of GPX4 after genipin intervention in GBM cells. (D) Changes in the protein level of ACSL4 after genipin intervention in GBM cells following changes in the ACSL4 protein level. $^{**}P < 0.01$, $^{***}P < 0.001$.

Discussion

Currently, the available treatment options for gliomas, such as imaging tests, surgical resection, radiation therapy, and chemotherapy, have limited efficacy and significant side effects [38–40]. Despite receiving treatment, the survival rate of glioma patients remains low [41]. Therefore, identifying suitable treatments for glioma is crucial. In this study, we discovered that a small molecule inhibitor called genipin can effectively inhibit tumor growth by

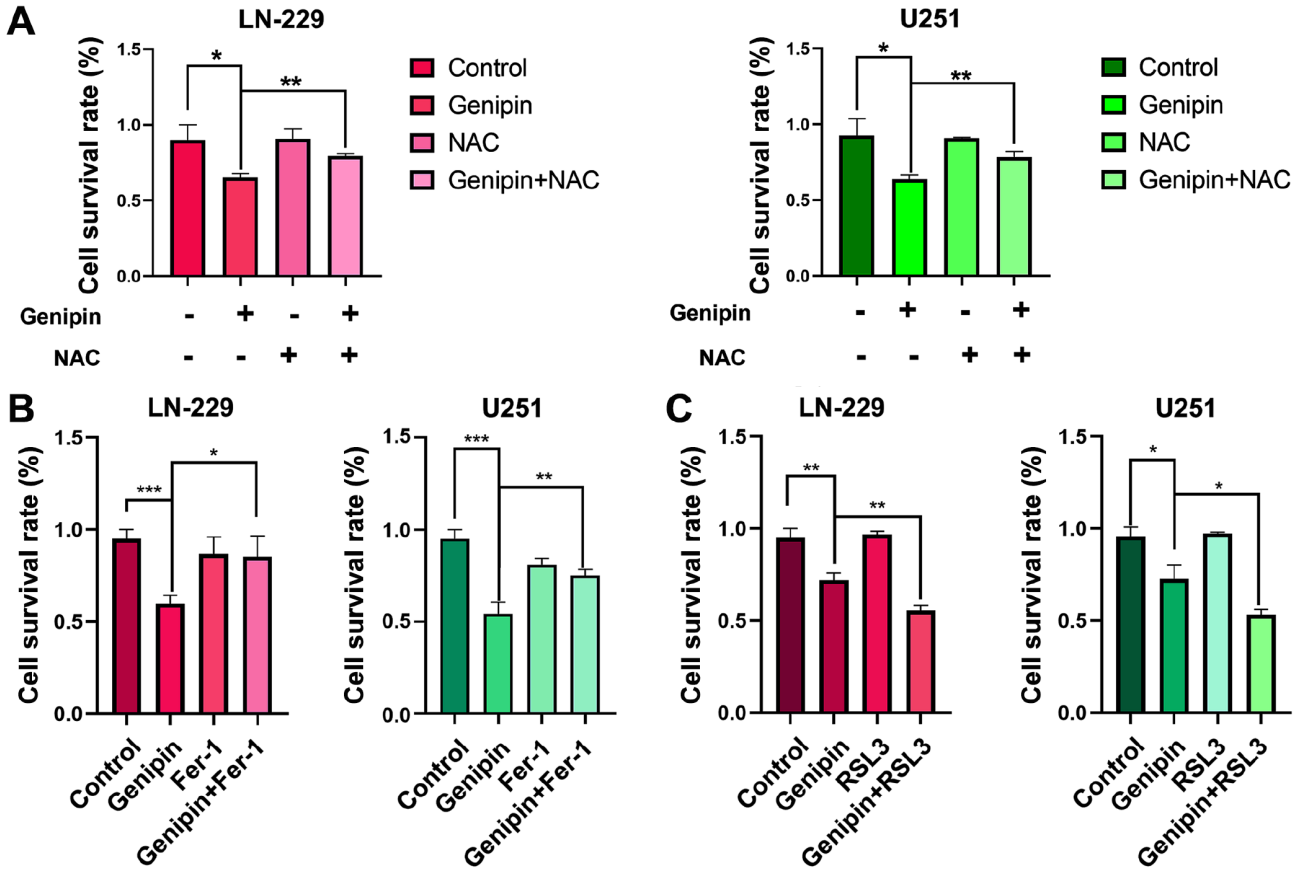

Figure 5. Genipin induces ferroptosis by increasing ROS in GBM cells (A) Effect of NAC on the viability of GBM cells. (B) Fer-1 rescues GBM cells from ferroptosis. (C) RSL3 exacerbates ferroptosis in GBM cells. *$P < 0.05$, **$P < 0.01$, ***$P < 0.001$.

suppressing the expression of UCP2 in GBM cells. We further demonstrated that through UCP2 inhibition, genipin can downregulate the expression of GPX4, a negative regulator of ferroptosis, and upregulate the expression of ACSL4, a positive regulator of ferroptosis, ultimately leading to ferroptosis (Figure 7). These findings suggest that genipin treatment based on UCP2 targeting has potential therapeutic applications with a clinical perspective for the treatment of GBM patients.

First, we found that UCP2 is highly expressed in tumor tissues and that its high expression is usually associated with poor prognosis. Our experiments verified that UCP2 is highly expressed in GBM cells. Since UCP2 plays a vital role in GBM proliferation, we attempted to identify a UCP2 inhibitor. Given the complexity of GBM, medication is certainly a good option. Current clinical studies have shown that the small-molecule inhibitor genipin can significantly inhibit UCP2. Genipin is a glycoside of gardenia glycosides that is often used as an anti-inflammatory agent.

Genipin, derived from the Gardenia jasminoides plant, has traditionally been used for its antipyretic, vasodilatory, and blood flow-improving effects[42]. Previous studies have shown that genipin inhibits UCP2-mediated proton leakage and reverses β-cell dysfunction induced by high glucose in isolated islets [43]. It has been demonstrated that genipin binds to arginine residues in UCP2, resulting in reduced proton transport in the presence of long-chain fatty acids [44].

To elucidate the mechanism underlying the potent inhibition of GBM cell growth by genipin, we conducted further studies. Initially, we discovered that UCP2 is a conserved protein located in the inner mitochondrial membrane. It is responsible for causing mitochondrial proton leakage, and its activity can be regulated by specific activators, such as reactive oxygen species (ROS). The activation of UCP2 leads to mitochondrial uncoupling and changes in membrane potential [45]. Alterations in the mitochondrial membrane potential can reduce mitochondrial ATP production. Conversely, changes in the mitochondrial membrane potential can induce mild uncoupling, which inhibits the mitochondrial production of ROS. It is evident that UCP2 plays a role in regulating ROS levels in cells [46]. Genipin inhibits UCP2, thereby preventing UCP2-mediated proton leakage (Figure 4A). This inhibition may enable a new role for ROS. Additionally, ROS are widely recognized as positive regulatory factors in ferroptosis. On the basis of the above information, we hypothesized that inhibition of UCP2 by genipin could affect the mitochondrial membrane potential and increase ROS production. Consequently, this process could trigger ferroptosis in GBM cells, thereby alleviating glioma development. Therefore, we conclude that the inhibition of UCP2 is a promising strategy for inducing ferroptosis through ROS accumulation.

Interestingly, we discovered that genipin induces ferroptosis by downregulating GPX4 and increasing ACSL4 protein levels. Ferroptosis is a unique form of cell death that is triggered by iron-dependent lipid peroxidation and is distinct from other programmed cell death modalities. A previous study highlighted the importance of ACSL4 and GPX4 as novel predictive and prognostic biomarkers for

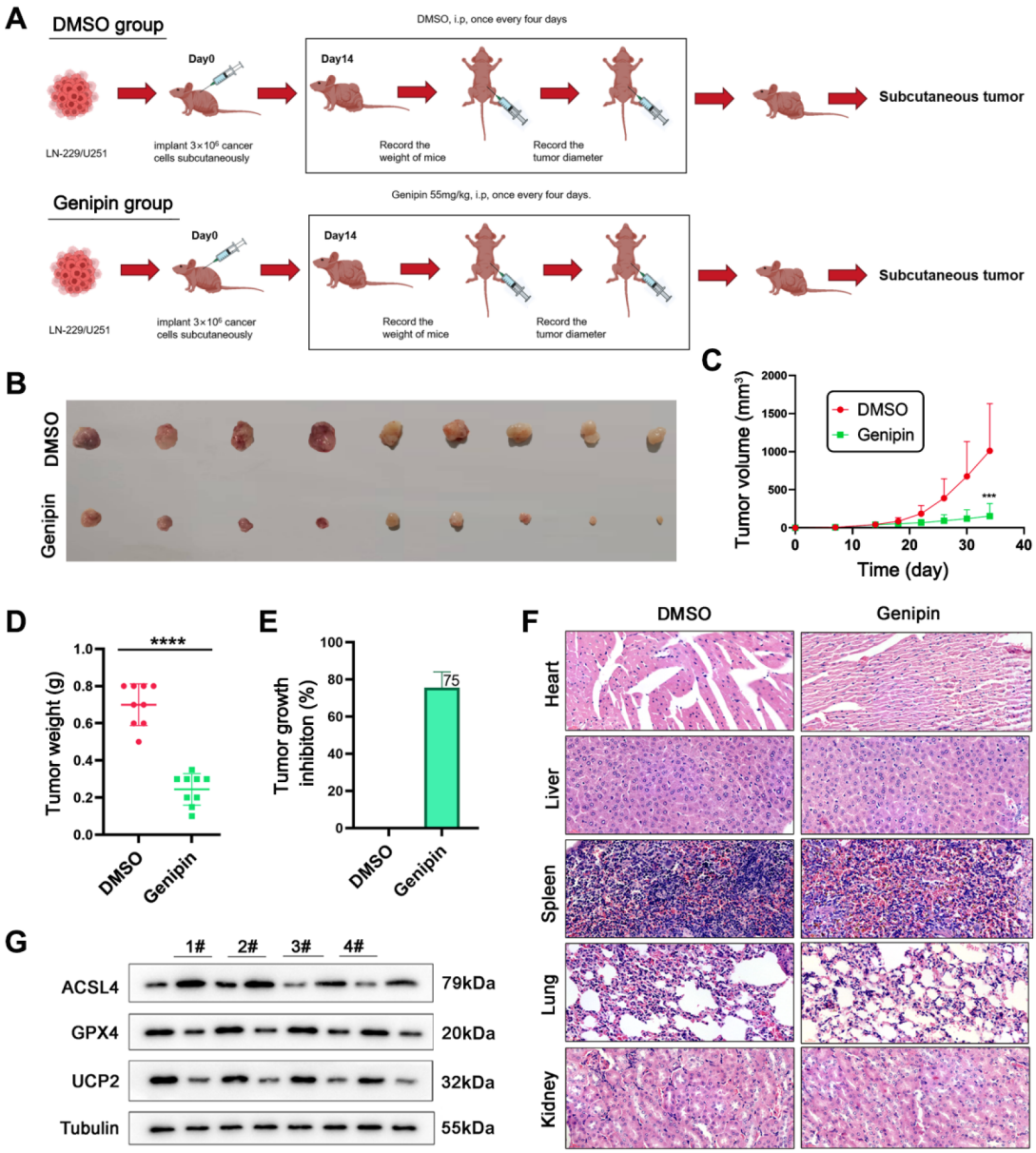

Figure 6. Genipin inhibits tumor growth *in vivo* in xenografts of GBM patient origin (A) Animal simulation experiment of the genipin manipulation process on subcutaneous gliomas. (B) Images of different tumors in the DMSO and genipin groups (split into two operations). (C) Changes in the average tumor volume of different groups of model mice treated with genipin ($n = 9$). (D) Tumor weights of the different groups of model mice after genipin treatment. (E) The tumor growth inhibition in the genipin group was greater than that in the DMSO group. (F) HE staining of other organs in mice after genipin treatment. (G) Four groups of tumor tissues were selected to evaluate the protein expressions of GPX4, ACSL4, and UCP2. ****$P < 0.0001$.

neoadjuvant chemotherapy. This study demonstrated that the interaction between ACSL4 and GPX4 can induce ferroptosis in breast cancer cells. While there is a significant body of literature on ferroptosis in cancer therapy, its application in GBM patients is limited. Our study revealed that genipin, which is traditionally used for inflammation treatment, effectively inhibits GBM development by inducing ferroptosis both *in vivo* and *in vitro*. Importantly, the results obtained from the effects of genipin intervention on UCP2, along with the use of NAC (an ROS inhibitor), further validated the occurrence of ferroptosis. To strengthen our confidence in the occurrence of ferroptosis, we conducted experiments using RSL3 (a ferroptosis inducer) and Fer-1 (a ferroptosis inhibitor) in treated glioma cells, the results of which were consistent with our previous experiments, confirming the occurrence of ferroptosis. Therefore, genipin treatment holds promise as a novel therapeutic approach for GBM patients.

In conclusion, UCP2 is a significant predictor of poor prognosis in GBM patients and can be considered a potential therapeutic target for GBM. Importantly, the targeting of UCP2 by genipin effectively inhibits GBM malignant behaviors through the induction of ferroptosis both *in vivo* and *in vitro*. These findings indicate that genipin treatment based on UCP2 targeting has potential therapeutic applications with a clinical perspective for the treatment of GBM patients.

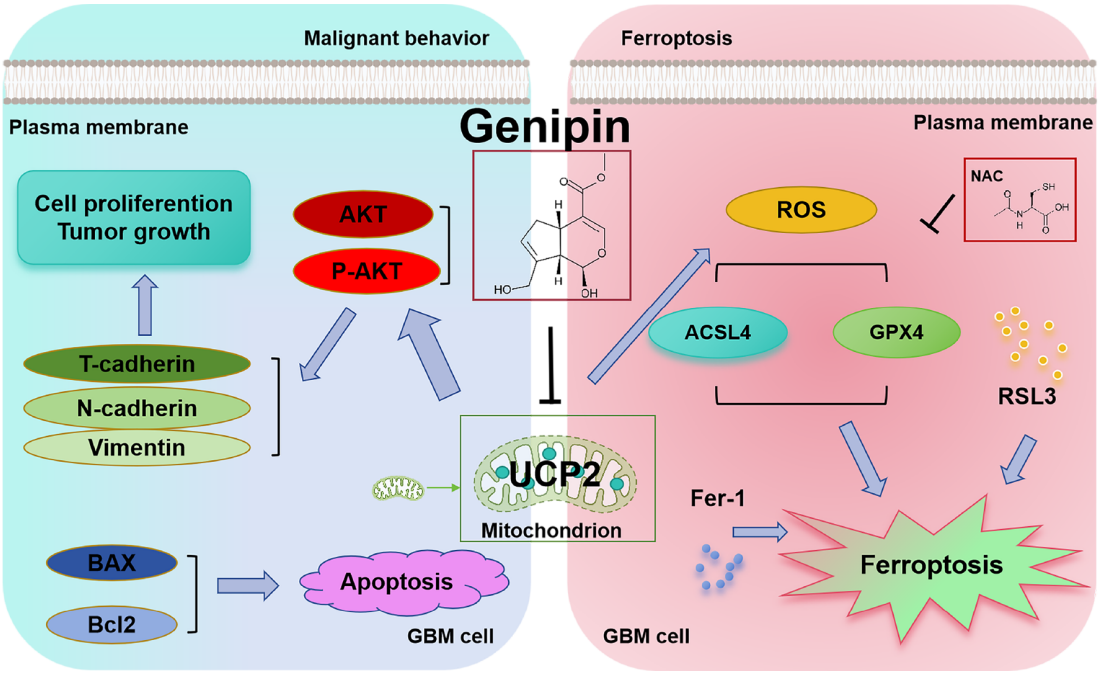

Figure 7. Schematic illustration of the suppression of malignant behavior and increased ferroptosis of GBM tumors with genipin targeting UCP2 Genipin inhibition of UCP2 results in changes in various malignant behaviors of GBM cells while inducing apoptosis in GBM, which together slow the growth of tumor cells (left). Genipin inhibition of UCP2 results in changes in the mitochondrial membrane potential, which acts concurrently with changes in the levels of ROS, which then decreases GPX4 level and increases the level of ACSL4 protein. Genipin induces iron-dependent and GPX4-mediated ferroptosis, which is closely related to ROS induction (right).

Supplementary Data

Supplementary data is available at *Acta Biochimica et Biophysica Sinica* online.

Funding

This work was supported by the grants from the National Natural Science Foundation of China (Nos. 82373124, 81872163, 82101410, and 81672631), the Natural Science Foundation of Shandong Province (No. ZR2023MH073), and the Health Science and Technology Development Plan Project of Shandong (No. 202101040805).

Conflict of Interest

The authors declare that they have no conflict of interest.

References

1. Wang LM, Englander ZK, Miller ML, Bruce JN. Malignant glioma. *Adv Exp Med Biol* 2023, 1405: 1–30
2. Xu S, Tang L, Li X, Fan F, Liu Z. Immunotherapy for glioma: current management and future application. *Canc Lett* 2020, 476: 1–12
3. Mahajan S, Schmidt MHH, Schumann U. The glioma immune landscape: a double-edged sword for treatment regimens. *Cancers* 2023, 15: 2024
4. Cai J, Hu Y, Ye Z, Ye L, Gao L, Wang Y, sun Q, *et al.* Immunogenic cell death-related risk signature predicts prognosis and characterizes the tumour microenvironment in lower-grade glioma. *Front Immunol* 2022, 13: 1011757
5. Nicholson JG, Fine HA. Diffuse glioma heterogeneity and its therapeutic implications. *Canc Discov* 2021, 11: 575–590
6. He X, Zhou Y, Chen W, Zhao X, Duan L, Zhou H, Li M, *et al.* Repurposed pizotifen malate targeting NRF2 exhibits anti-tumor activity through inducing ferroptosis in esophageal squamous cell carcinoma. *Oncogene* 2023, 42: 1209–1223
7. Zhao R, Jiang S, Zhang L, Yu Z. Mitochondrial electron transport chain, ROS generation and uncoupling (Review). *Int J Mol Med* 2019, 44: 3–15
8. Carrageta DF, Freire-Brito L, Guerra-Carvalho B, Bernardino RL, Monteiro BS, Barros A, Oliveira PF, *et al.* Mitochondrial uncoupling proteins regulate the metabolic function of human sertoli cells. *Reproduction* 2023, 167: e230229
9. Kumar R, T A, Singothu S, Singh SB, Bhandari V. Uncoupling proteins as a therapeutic target for the development of new era drugs against neurodegenerative disorder. *Biomed Pharmacother* 2022, 147: 112656
10. Li J, Jiang R, Cong X, Zhao Y. UCP 2 gene polymorphisms in obesity and diabetes, and the role of UCP 2 in cancer. *FEBS Lett* 2019, 593: 2525–2534
11. Forte M, Bianchi F, Cotugno M, Marchitti S, Stanzione R, Maglione V, Sciarretta S, *et al.* An interplay between UCP2 and ROS protects cells from high-salt-induced injury through autophagy stimulation. *Cell Death Dis* 2021, 12: 919
12. Zhao P, Li X, Yang Q, Lu Y, Wang G, Yang H, Dong J, *et al.* Malvidin alleviates mitochondrial dysfunction and ROS accumulation through activating AMPK-α/UCP2 axis, thereby resisting inflammation and apoptosis in SAE mice. *Front Pharmacol* 2023, 13: 1038802
13. Vallejo FA, Vanni S, Graham RM. UCP2 as a potential biomarker for adjunctive metabolic therapies in tumor management. *Front Oncol* 2021, 11: 640720
14. Tutunchi H, Ostadrahimi A, Saghafi-Asl M, Hosseinzadeh-Attar MJ, Shakeri A, Asghari-Jafarabadi M, Roshanravan N, *et al.* Oleoylethanolamide supplementation in obese patients newly diagnosed with non-alcoholic fatty liver disease: effects on metabolic parameters, anthropometric indices, and expression of PPAR-α, UCP1, and UCP2 genes. *Pharmacol Res* 2020, 156: 104770

15. Segalés J, Sánchez-Martín C, Pujol-Morcillo A, Martín-Ruiz M, de los Santos P, Lobato-Alonso D, Oliver E, *et al.* Role of UCP2 in the energy metabolism of the cancer cell line A549. *Int J Mol Sci* 2023, 24: 8123
16. Du W, Yin F, Zhong Y, Luo M, Wang Z, Lin P, Liu Q, *et al.* CircUCP2 promotes the tumor progression of non-small cell lung cancer through the miR-149/UCP2 pathway. *Oncol Res* 2023, 31: 929–936
17. Oliveira MS, Rheinheimer J, Moehlecke M, Rodrigues M, Assmann TS, Leitão CB, Trindade MRM, *et al.* UCP2, IL18, and miR-133a-3p are dysregulated in subcutaneous adipose tissue of patients with obesity. *Mol Cell Endocrinol* 2020, 509: 110805
18. Lee S, Moon H, Kim G, Cho JH, Dae-Hee L, Ye MB, Park D. Anion transport or nucleotide binding by Ucp2 is indispensable for Ucp2-mediated efferocytosis. *Molecules Cells* 2015, 38: 657–662
19. Echtay KS, Winkler E, Frischmuth K, Klingenberg M. Uncoupling proteins 2 and 3 are highly active H^+ transporters and highly nucleotide sensitive when activated by coenzyme Q (ubiquinone). *Proc Natl Acad Sci USA* 2001, 98: 1416–1421
20. Nagao Y, Yokoi A, Yoshida K, Sugiyama M, Watanabe E, Nakamura K, Kitagawa M, *et al.* Novel therapeutic strategies targeting UCP2 in uterine leiomyosarcoma. *Pharmacol Res* 2023, 189: 106693
21. Luby A, Alves-Guerra MC. UCP2 as a cancer target through energy metabolism and oxidative stress control. *Int J Mol Sci* 2022, 23: 15077
22. Yu X, Shi M, Wu Q, Wei W, Sun S, Zhu S. Identification of UCP1 and UCP2 as potential prognostic markers in breast cancer: a study based on immunohistochemical analysis and bioinformatics. *Front Cell Dev Biol* 2022, 10: 891731
23. Cheng WC, Tsui YC, Ragusa S, Koelzer VH, Mina M, Franco F, Läubli H, *et al.* Uncoupling protein 2 reprograms the tumor microenvironment to support the anti-tumor immune cycle. *Nat Immunol* 2019, 20: 206–217
24. Ahmed R, ul ain Hira N, Wang M, Iqbal S, Yi J, Hemar Y. Genipin, a natural blue colorant precursor: source, extraction, properties, and applications. *Food Chem* 2024, 434: 137498
25. Donovan C, Sun M, Cogswell D, Margo CE, Avila MY, Espana EM. Genipin increases extracellular matrix synthesis preventing corneal perforation. *Ocular Surf* 2023, 28: 115–123
26. Utami Nike D, Md Fadilah NI, Sallehuddin N, Nor Azlan AYH, Imran FH, Maarof M, Fauzi MB. Genipin-crosslinking effects on biomatrix development for cutaneous wound healing: a concise review. *Front Bioeng Biotechnol* 2022, 10: 865014
27. Cho YS. Genipin, an inhibitor of UCP2 as a promising new anticancer agent: a review of the literature. *Int J Mol Sci* 2022, 23: 5637
28. Zhao B, Sun L, Jiang X, Zhang Y, Kang J, Meng H, Li H, *et al.* Genipin protects against cerebral ischemia-reperfusion injury by regulating the UCP2-SIRT3 signaling pathway. *Eur J Pharmacol* 2019, 845: 56–64
29. Zeng F, Nijiati S, Tang L, Ye J, Zhou Z, Chen X. Ferroptosis detection: from approaches to applications. *Angew Chem Int Ed* 2023, 62: e202300379
30. Costa I, Barbosa DJ, Benfeito S, Silva V, Chavarria D, Borges F, Remião F, *et al.* Molecular mechanisms of ferroptosis and their involvement in brain diseases. *Pharmacol Ther* 2023, 244: 108373
31. Xu L, Liu Y, Chen X, Zhong H, Wang Y. Ferroptosis in life: to be or not to be. *Biomed Pharmacother* 2023, 159: 114241
32. Lin Q, Li S, Jin H, Cai H, Zhu X, Yang Y, Wu J, *et al.* Mitophagy alleviates cisplatin-induced renal tubular epithelial cell ferroptosis through ROS/HO-1/GPX4 axis. *Int J Biol Sci* 2023, 19: 1192–1210
33. Zhang S, Liu Q, Chang M, Pan Y, Yahaya BH, Liu Y, Lin J. Chemotherapy impairs ovarian function through excessive ROS-induced ferroptosis. *Cell Death Dis* 2023, 14: 340
34. Yang F, Xiao Y, Ding JH, Jin X, Ma D, Li DQ, Shi JX, *et al.* Ferroptosis heterogeneity in triple-negative breast cancer reveals an innovative immunotherapy combination strategy. *Cell Metab* 2023, 35: 84–100.e8
35. Yan H, Talty R, Johnson CH. Targeting ferroptosis to treat colorectal cancer. *Trends Cell Biol* 2023, 33: 185–188
36. Wang D. Progress in the study of ferroptosis in cancer treatment: state-of-the-Art. *Chem Biol Interact* 2023, 371: 110348
37. Li Z, Li X, He X, Jia X, Zhang X, Lu B, Zhao J, *et al.* Proteomics reveal the inhibitory mechanism of levodopa against esophageal squamous cell carcinoma. *Front Pharmacol* 2020, 11: 568459
38. Śledzińska P, Bebyn M, Furtak J, Koper A, Koper K. Current and promising treatment strategies in glioma. *Rev Neuroscis* 2023, 34: 483–516
39. Qiu Q, Ding X, Chen J, Chen S, Wang J. Nanobiotechnology-based treatment strategies for malignant relapsed glioma. *J Control Release* 2023, 358: 681–705
40. Keluth S, Jitte S, Bhushan R, Ranjan OP, Murti K, Ravichandiran V, Kumar N. Targeting ion channels for the treatment of glioma. *Mini Rev Med Chem* 2023, 23: 1298–1318
41. Wang J, Qi F, Wang Z, Zhang Z, Pan N, Huai L, Qu S, *et al.* A review of traditional Chinese medicine for treatment of glioblastoma. *Biosci Trends* 2019, 13: 476–487
42. Li M, Wang K, Wang Y, Han Q, Ni Y, Wen X. Effects of genipin concentration on cross-linked β-casein micelles as nanocarrier of naringenin: colloidal properties, structural characterization and controlled release. *Food Hydrocolloids* 2020, 108: 105989
43. Zhang CY, Parton LE, Ye CP, Krauss S, Shen R, Lin CT, Porco Jr JA, *et al.* Genipin inhibits UCP2-mediated proton leak and acutely reverses obesity- and high glucose-induced β cell dysfunction in isolated pancreatic islets. *Cell Metab* 2006, 3: 417–427
44. Kreiter J, Rupprecht A, Zimmermann L, Moschinger M, Rokitskaya TI, Antonenko YN, Gille L, *et al.* Molecular mechanisms responsible for pharmacological effects of genipin on mitochondrial proteins. *Biophys J* 2019, 117: 1845–1857
45. Schiffer TA, Löf L, Gallini R, Kamali-Moghaddam M, Carlström M, Palm F. Mitochondrial respiration-dependent ANT2-UCP2 interaction. *Front Physiol* 2022, 13: 866590
46. Yu J, Shi L, Lin W, Lu B, Zhao Y. UCP2 promotes proliferation and chemoresistance through regulating the NF-κB/β-catenin axis and mitochondrial ROS in gallbladder cancer. *Biochem Pharmacol* 2020, 172: 113745